Modified Halocline Water over the Laptev Sea Continental Margin: Historical Data Analysis

IGOR A. DMITRENKO

Centre for Earth Observation Science, University of Manitoba, Winnipeg, Manitoba, Canada

SERGEY A. KIRILLOV

Arctic and Antarctic Research Institute, St. Petersburg, Russia

VLADIMIR V. IVANOV*

Arctic and Antarctic Research Institute, St. Petersburg, Russia, and International Arctic Research Center, University of Alaska Fairbanks, Fairbanks, Alaska

BERT RUDELS

Finnish Meteorological Institute, and Department of Physics, University of Helsinki, Helsinki, Finland

NUNO SERRA AND NIKOLAY V. KOLDUNOV

Institute of Oceanography, University of Hamburg, Hamburg, Germany

(Manuscript received 14 June 2011, in final form 16 December 2011)

ABSTRACT

Historical hydrographic data (1940s–2010) show a distinct cross-slope difference of the lower halocline water (LHW) over the Laptev Sea continental margins. Over the slope, the LHW is on average warmer and saltier by 0.2°C and 0.5 psu, respectively, relative to the off-slope LHW. The LHW temperature time series constructed from the on-slope historical records are related to the temperature of the Atlantic Water (AW) boundary current transporting warm water from the North Atlantic Ocean. In contrast, the on-slope LHW salinity is linked to the sea ice and wind forcing over the potential upstream source region in the Barents and northern Kara Seas, as also indicated by hydrodynamic model results. Over the Laptev Sea continental margin, saltier LHW favors weaker salinity stratification that, in turn, contributes to enhanced vertical mixing with underlying AW.

1. Introduction

The halocline layer (HL) of the Arctic Ocean represents a transition between two water masses: cold, fresh surface mixed water and the warm and saltier intermediate Atlantic Water (AW) layer beneath, with the lower part of the HL—low halocline water (LHW)—centered around isohaline 34.2 psu (e.g., Coachman and Aagaard 1974). The HL is vertically stratified in salinity, and the associated density gradient suppresses the upward heat flux to the sea surface from the underlying warmer intermediate AW. Given the recent increase of temperature in the AW layer over the Eurasian continental margin (e.g., Dmitrenko et al. 2008), understanding the formation, spreading, and modification of the overlaying LHW is important in predicting how the Arctic Ocean may respond to climate change.

There has been general agreement on the fact that the LHW over the Eurasian Basin is conditioned by advection from the northern Kara and Barents Seas and

* Additional affiliation: Scottish Marine Institute, Oban, United Kingdom.

Corresponding author address: Igor A. Dmitrenko, Centre for Earth Observation Science, University of Manitoba, Wallace Bldg., 125 Dysart Rd., Winnipeg, Manitoba R3T 2N2, Canada.
E-mail: dmitreni@cc.umanitoba.ca

DOI: 10.1175/JCLI-D-11-00336.1

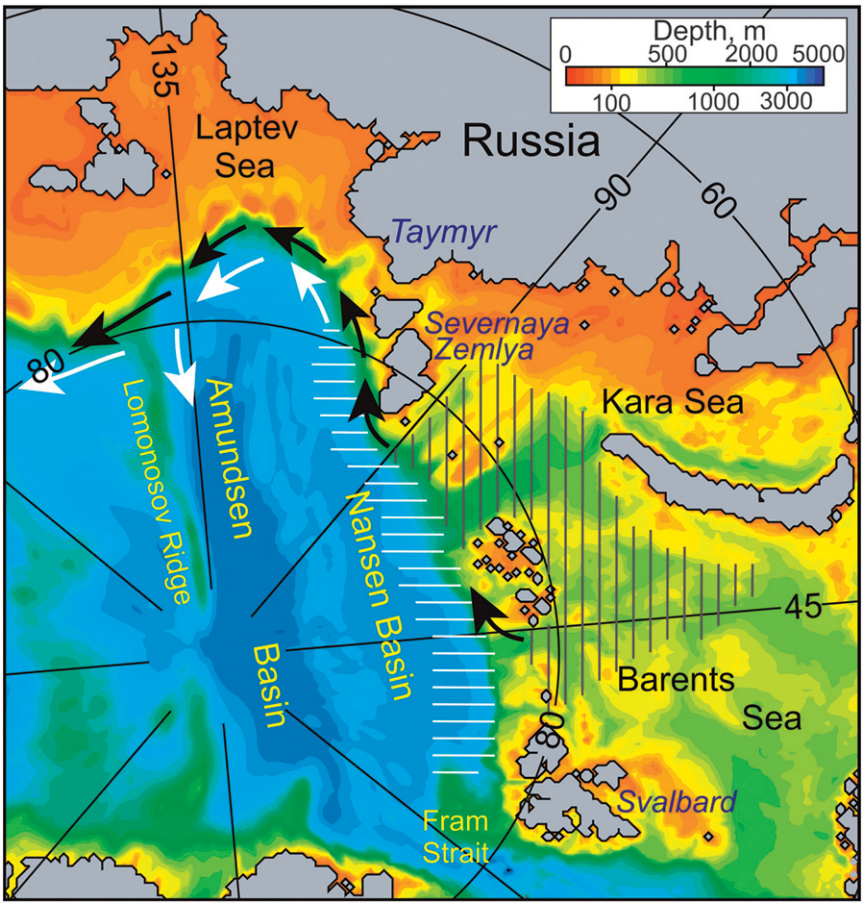

FIG. 1. A map of the eastern Arctic Ocean. The schematic shows the formation area (shading) and the circulation (arrows) of the Fram Strait branch halocline (white) and the Barents Sea branch halocline (black), following Rudels et al. (2004).

adjacent Nansen Basin (e.g., Steele et al. 1995; Rudels et al. 1996, 2004). The on-slope LHW over the Eurasian continental slope is believed to be a part of the Barents Sea branch entering the Arctic Ocean in the northern Kara Sea through St. Anna Trough, and the Fram Strait branch controls the off-slope LHW over the Nansen Basin downstream of the mouth of St. Anna Trough (Fig. 1; Rudels et al. 2004). In addition, the LHW of the Barents Sea branch is more saline. The reason is that the AW in the Barents Sea has become cooled before it encounters sea ice. The sea ice melting, which is due to interaction with a cooler AW in the Barents Sea, leads to a higher upper-layer salinity than the corresponding melting occurring north of Svalbard, where the warmer Fram Strait branch enters the Arctic Ocean and meets sea ice (Fig. 1; Rudels et al. 2004; Rudels 2010). This favors stronger downstream vertical mixing with warmer AW occurring at the Eurasian continental slope. Expanding on these suggestions, the work presented here focuses on the modification of the LHW over the continental slope of the Laptev Sea (Fig. 1), with the aim of explaining the differences in the thermohaline properties between the on- and off-slope LHW. In particular, we build on a recent report by Dmitrenko et al. (2011) that shows the LHW modified over the Laptev Sea continental slope by vertical mixing with underlying AW. Here, we look at the properties of the LHW over the Laptev Sea continental slope and adjacent Eurasian Basin derived from historical hydrographic data from the 1940s to 2010. More specifically, our study focuses on 1) local on-slope modification of the LHW due to interaction with underlying AW and 2) remote modifications imposed upstream by sea ice and atmospheric forcing by conducting statistical analysis of historical data.

2. Data and methods

Our historical hydrographic data comprise different datasets from the 1940s to 1990, previously used for the Arctic Climatology Project (1997, 1998) atlas of the

Arctic Ocean. These datasets were updated with observations of the 1990s–2000s and recent data obtained under the working frame of the International Polar Year Project in 2007–09. The majority of the winter hydrographic data came from the Soviet aircraft surveys in 1963–88 when the AW boundary current demonstrated a negative temperature and salinity anomaly (Polyakov et al. 2004). In contrast, the majority of the summer data represent two periods of warmer and saltier AW from the 1950s and from 1990 to 2010 (Polyakov et al. 2003, 2004; Dmitrenko et al. 2008). For the upper AW (150–250 m) in the central Laptev Sea, this results in artificial bias between the long-term mean summer and winter temperatures and salinities by 0.65°C and 0.1 psu, respectively, that is not associated with naturally driven seasonality.

In the following, the LHW characteristics are taken to be those observed between 45 and 55 m on the basis of the long-term mean on-slope and off-slope vertical temperature and salinity profiles at ~126°E (Figs. 2a and 2b), the central region in our domain of interest over the Laptev Sea continental slope (Fig. 1). By this definition, the LHW is characterized by an intermediate temperature minimum between the overlaying warmer surface layer heated by solar radiation during summer and the underlying warmer AW (Fig. 2b). Our approach for comparing LHW spatial patterns along the fixed depth of the intermediate temperature minimum is preferred over other potential methods such as analyzing the data along the LHW density range. The reason is that on-slope and off-slope LHW thermohaline properties are different, with saltier and warmer on-slope LHW and fresher and cooler off-slope LHW (Figs. 2a and 2b), and with the on-slope LHW being initially denser. For the depth range of the off-slope temperature minimum, we analyze both cross-slope temperature and salinity (density) differences. In contrast, for the density range of the off-slope temperature minimum, only the temperature difference is significant, but the salinity difference is negligible (within the LHW range of temperatures and salinities, the density is mainly driven by salinity). The upper AW layer is defined between 150 and 250 m (Figs. 2c and 2d).

The long-term mean LHW temperature and salinity over the Laptev Sea continental slope and adjacent Arctic Ocean are compiled to assess the background spatial patterns of the LHW. For each year from the 1940s to 2010, summer and winter historical temperature and salinity measurements in the LHW layer were linearly interpolated using data from a 50-km search radius onto a regular grid with a horizontal resolution of 20 km (Figs. 3d and 3h). The long-term mean LHW temperature and salinity with their standard deviations were computed at each node of the regular grid (Figs. 3a–d). The same procedure was applied to obtain thermohaline characteristics for the upper AW (Figs. 3e–h). In addition, the 1940s–2010 time series of the LHW and upper AW temperature and salinity are calculated at ~126°E by integrating all measurements over the distance of 60 km from the grid nodes at 78.50°N (off slope) and 77.20°N (on slope; Figs. 3a and 3e). The continental slope at ~126°E provides more data than other regions, with on-slope LHW measurements taken for at least 25 years (Fig. 3d).

The long-term mean (1970–2009) LHW water velocity and salinity along the Laptev Sea continental margin were derived from numerical simulations at 50 m with the coupled ocean–sea ice Massachusetts Institute of Technology general circulation model (Marshall et al. 1997) configured for the Atlantic Ocean region north of 30°S, including the Nordic seas and the Arctic Ocean. The setup is a version of the model described in Serra et al. (2010) with a horizontal resolution of ~7.5 km. While the model is only eddy permitting in the Arctic Ocean, it is eddy resolving throughout the whole Atlantic Ocean. A more realistic Atlantic is thus assumed to lead to a more realistic Arctic, via more realistic properties of Arctic inflow, even if the Arctic Ocean part is only eddy permitting. The model is initialized from rest and with the annual mean temperature and salinity from the World Ocean Circulation Experiment Global Hydrographic Climatology (Gouretski and Koltermann 2004). The model is forced at the surface by the 1948–2009 6-hourly atmospheric state from the National Centers for Environmental Prediction (NCEP) "RA1" reanalysis (Kalnay et al. 1996), using bulk formulas.

The time series of winter-mean (January–April) meridional wind was calculated from the NCEP reanalysis near-surface wind fields (1948–2010) by averaging over the area from 75° to 77.5°N and from 120° to 130°E. The time series of winter-mean sea ice extent (SIE) and meridional wind over the Barents and northern Kara Seas are from Dmitrenko et al. (2009).

3. Results

The LHW temperature and salinity spatial distribution shows significant differences between the on-slope and off-slope regions (Fig. 3). Over the depth range of the LHW layer (45–55 m), we reveal cyclonic inflow of saltier water around the deep Eurasian Basin that primarily follows the Laptev Sea continental slope (Fig. 3c). The long-term mean LHW salinity exhibits spatial variability, gradually decreasing along margin from 34.1 near the Severnaya Zemlya Archipelago to 33.8 at ~126°E, 33.5 near the slope junction with the Lomonosov Ridge, and ~33 over the Eurasian flank of the Lomonosov Ridge (Fig. 3c). Cross margin, the maximum LHW salinities are traced over the slope following the depth contours 200–1000 m with the

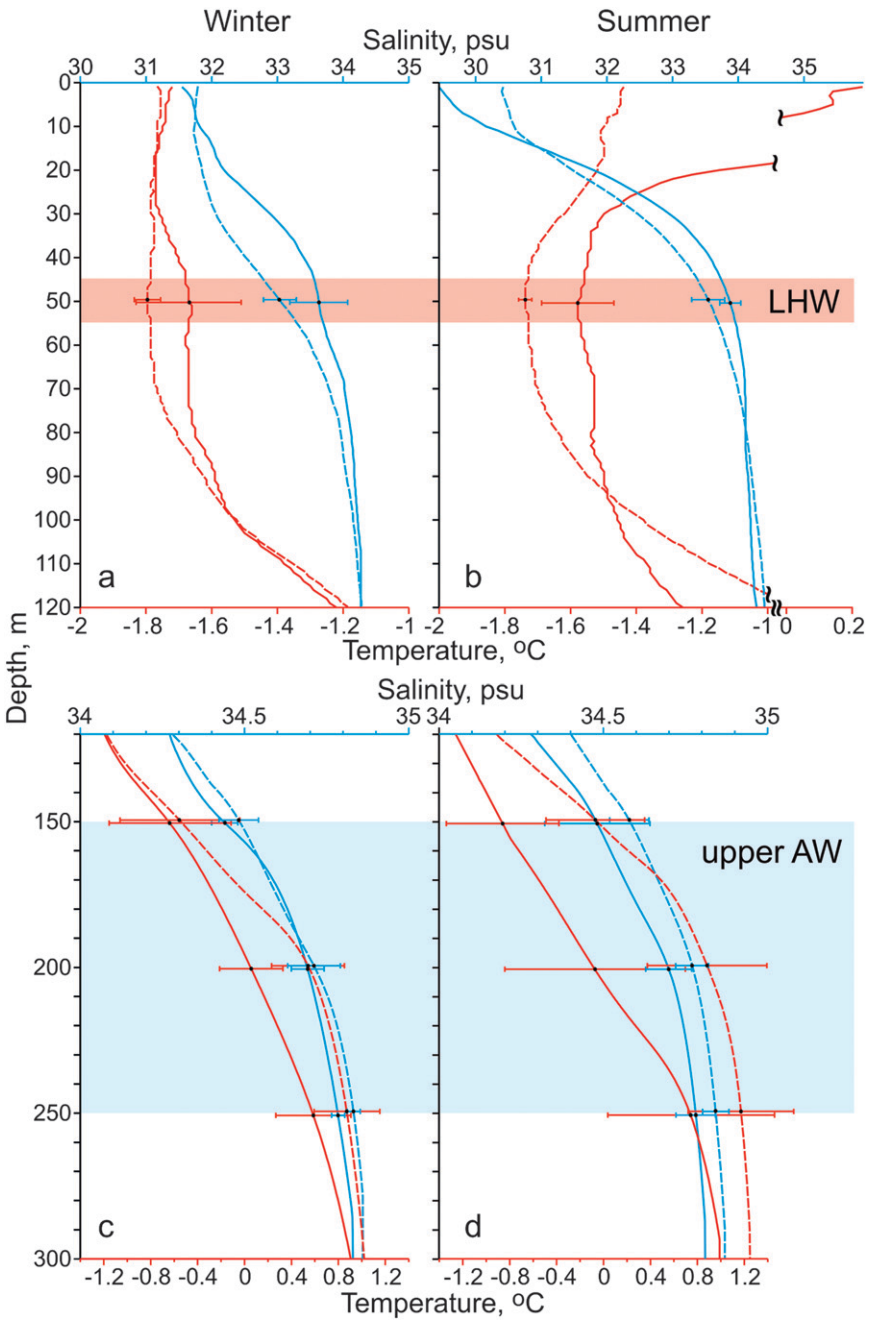

FIG. 2. The long-term mean (1940s–2010) vertical profiles of temperature (°C; red) and salinity (psu; blue) at 77.20°N (on slope; solid lines) and 78.50°N (off slope; dashed lines) in the central Laptev Sea at ~126°E (for geographical positions, see Figs. 3a and 3e) for (left) winter and (right) summer. The error bars show ±1 standard deviation of the mean. Pink and blue shadings indicate the depth range for the (top) LHW and (bottom) upper AW, respectively.

maximum salinity on slope exceeding the off-slope salinities by 0.50–0.75 psu (Fig. 3c). The LHW salinity standard deviation is relatively uniform (at ~0.2 psu), tending to increase toward the western flank of the Lomonosov Ridge (Fig. 3d). The long-term mean LHW temperature shows relatively warmer water up to −1.5°C on slope (shallower than 1000 m); off slope (deeper than 1500–2000 m) the LHW temperature is lower, between −1.7 and −1.8°C (Fig. 3a). In contrast to salinity, the LHW temperature standard deviation increases from less than

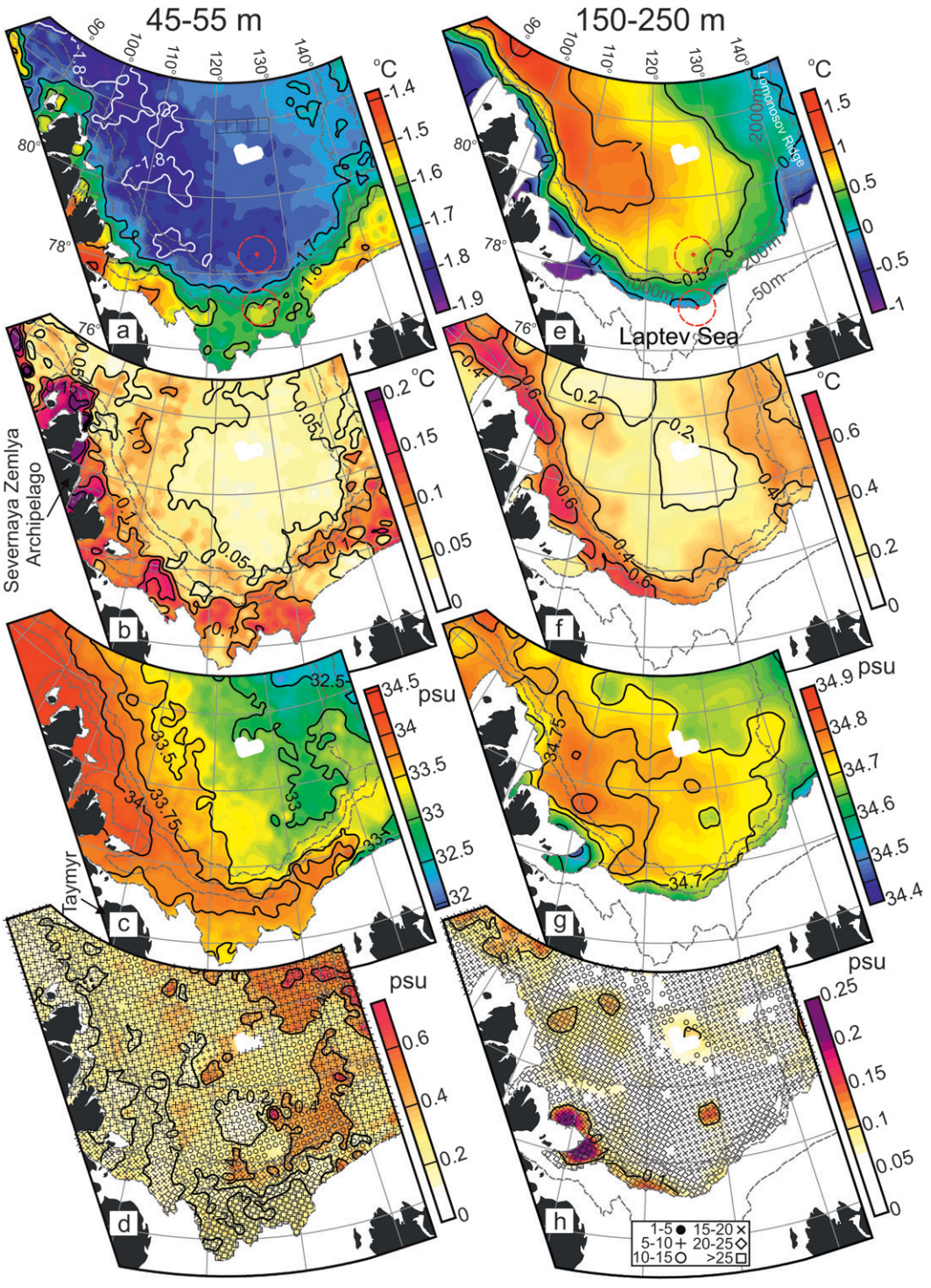

FIG. 3. The gridded long-term mean (1940s–2010) thermohaline characteristics for (left) LHW (45–55 m) and (right) upper AW (150–250 m) over the Siberian sector of the Arctic Ocean Eurasian Basin. (a),(e) Temperature with (b),(f) standard deviations (°C), and (c),(g) salinity with (d),(h) standard deviations (psu). Dashed lines show 50-, 200-, 1000-, and 2000-m depth contours. In (d) and (h), symbols depict grid nodes, with number of data-covered years defined by symbol code in the legend on the bottom of (h). Red crosses in (a) and (e) show grid nodes where the long-term mean profiles (Fig. 2) and the time series (Fig. 4) for the LHW and upper AW are compiled by averaging all data over the on-slope and off-slope areas delimited by red dashed circles.

0.1°C over the central basin to more than 0.15°C toward the basin margins (Fig. 3b). The upper AW (Fig. 3, right) shows patterns that are generally similar to those of the LHW, but the core of the AW boundary current roughly traced by the 1°C isotherm is displaced off slope by 150–200 km (Fig. 3e).

The LHW and AW temperature and salinity time series at ~126°E show characteristic features of the interannual variability. The on-slope LHW temperature exhibits two relatively warm periods, in the 1950s and in the 1990s–2000s, and one cold period in the 1960s–80s (Fig. 4c). The same warmer and cooler periods stand out over the AW core temperature anomalies shown by Polyakov et al. (2004). In contrast, the off-slope LHW temperature demonstrates low interannual variability with the temperature standard deviation lowered by a factor of 4 (not shown). The on-slope LHW temperature variability is in phase with the off-slope AW temperature variability (Figs. 4b,c). In fact, a positive correlation is found between the on-slope LHW temperature and off-slope AW temperature (coefficient $r = 0.64$) and off-slope AW salinity ($r = 0.65$, not shown). This correlation (and others presented later) is statistically significant at the 95% confidence level. Note that no smoothing or any kind of data corrections have been applied to the data in Fig. 4. Furthermore, the on-slope LHW temperature negatively correlates with the depth of the AW-layer upper boundary ($r = -0.61$; Figs. 4a,c) traced by the 0°C isotherm and calculated for the area between on-slope and off-slope locations at ~126°E (Fig. 3e). In addition, winter on-slope LHW temperature positively correlates with winter-mean meridional wind ($r = 0.55$; Figs. 4c,d) averaged over the central Laptev Sea continental slope. In contrast to the on-slope LHW temperature, the on-slope LHW salinity exhibits no correlation with any of the potential predictors from the Laptev Sea region, including off-slope AW temperatures and salinities and atmospheric vorticity, which controls the pathways of the Laptev Sea river runoff water. In contrast to the on-slope conditions, the off-slope LHW shows positively correlated temperatures and salinities ($r = 0.53$). The off-slope LHW temperature and salinity also correlate with those for the underlying upper AW ($r = 0.51$ for temperatures and $r = 0.42$ for salinities; not shown).

4. Discussion

In general, our historical data analysis (Fig. 3, left) confirms the consistent difference between the on-slope and off-slope LHW properties reported by Dmitrenko et al. (2011) for the cross-slope transect taken at ~126°E annually from 2002 to 2009, with warmer and saline on-slope LHW and cooler and fresher off-slope LHW. With the AW being the main source of heat over the Laptev Sea continental slope, positive correlation between the on-slope LHW and off-slope AW temperatures allows direct attribution of the on-slope LHW temperature variability to the AW. Following Dmitrenko et al. (2011), we suggest the enhanced on-slope vertical mixing between LHW and underlying AW to account for an important proportion of the difference between the on- and off-slope LHW temperatures. During the warm AW periods, the elevated AW boundary favors enhanced upward heat fluxes to the LHW, contributing to a positive LHW temperature anomaly (Figs. 4a–c).

The southerly winds, forcing over the Laptev Sea during winter, tend to facilitate vertical exchange, advecting more AW onto the slope. Mooring observations over the Laptev Sea continental slope at ~126° show the shift of the AW core toward the slope in winter and away from the slope in summer. Model simulation shows that seasonal variation of wind is among the possible factors governing seasonal changes of the AW layer (Dmitrenko et al. 2006), specifically during the cold AW period in the 1960s–1980s (Fig. 4d). The on-slope advection of the AW core elevates the AW boundary and increases the on-slope AW temperature. This, in turn, favors enhanced upward heat fluxes to the LHW. This is confirmed by positive correlation ($r = 0.51$) between the LHW temperature and the meridional (off slope) wind component during winter (Figs. 4c,d). Our correlation analysis also indicates that the off-slope LHW seems to be controlled by vertical exchange with underlying AW, as also follows from Polyakov et al. (2010). The enhanced on-slope vertical mixing is also consistent with a cross-slope difference in AW properties, with cooler and fresher on-slope AW and warmer and saline off-slope AW (Figs. 2c, 2d, 3e, and 3g).

Furthermore, Dmitrenko et al. (2011) obtained that at 126°E the mean (2002–09) on-slope LHW layer heat content increases by 48 ± 34 MJ m^{-2} relative to the off slope. Assuming a common upstream location for the on-slope and off-slope LHW as far away as ~1000 km upstream of our observational site (the area of confluence between two halocline branches in the northern Kara Sea; Fig. 1) and assuming the 2.5-yr travel time between the northern Kara Sea and the central Laptev Sea (~1.3 cm s^{-1}; Dmitrenko et al. 2008), one may obtain the on-slope vertical heat flux anomaly (on slope vs off slope) from the AW to the LHW of 0.61 ± 0.43 W m^{-2}. This estimate is consistent with an annual-mean upward heat flux anomaly (2007 vs climatology) across the LHW, enhanced on slope relative to the off slope by ~0.6 W m^{-2} on the basis of a 1D ocean column model simulation (Polyakov et al. 2010).

Complementing the recent report by Dmitrenko et al. (2011), the present analysis reveals no relationship

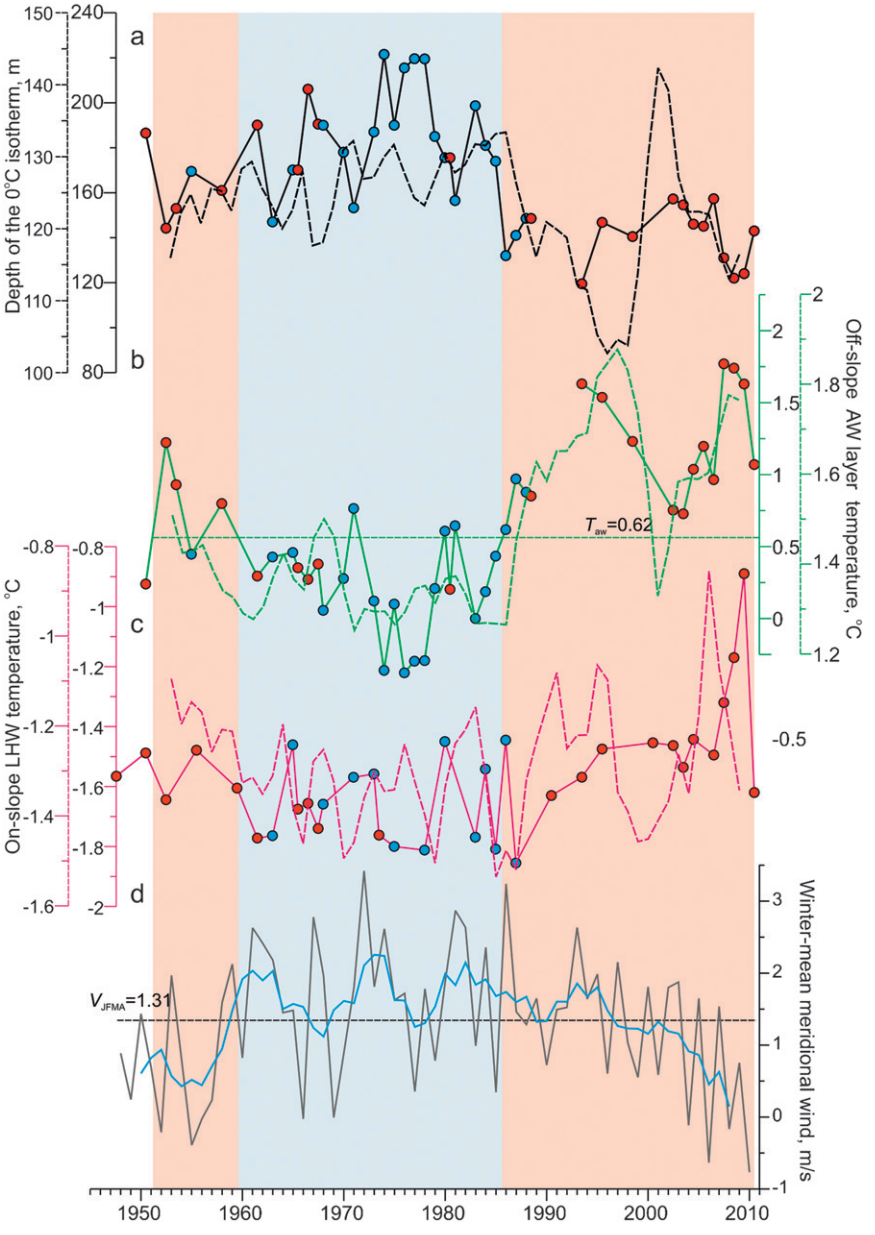

FIG. 4. Time series of (a) depth of the 0°C isotherm in the upper AW layer (black solid line), (b) temperatures for the off-slope upper AW (green solid line), and (c) temperature for the on-slope LHW (violet solid line) at ~126°E in comparison with those derived from a numerical simulation (dashed lines). Red and blue dots show summer and winter data, respectively. (d) Meridional surface wind averaged from January to April over the central Laptev Sea continental slope (gray line), and its 5-yr running mean (blue line). Horizontal dashed lines show the long-term mean for upper-AW temperature [in (b)] and meridional wind [in (d)]. Pink and blue shadings indicate positive and negative temperature anomalies, respectively, for the off-slope upper AW.

between the on-slope LHW salinity and potential local predictors. The stark difference in the patterns of temporal variance of the LHW temperature and salinity fields (Figs. 3b and 3d) also evidences that the salinity and temperature anomalies had distinct origins. These indicate the remote source of the on-slope LHW suggested by Rudels et al. (2004) and Rudels (2010) to be upstream in the Barents Sea, where the surface water is created by interaction between the AW inflow and sea ice (Fig. 1). The salinity obtained there (~34.5 psu) is the

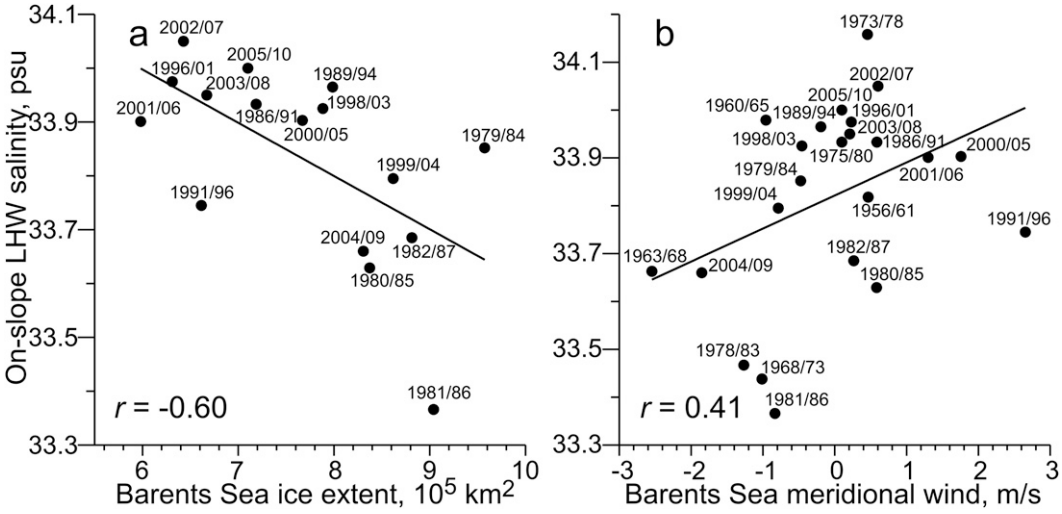

FIG. 5. The 5-yr lagged linear regression between the Laptev Sea on-slope LHW salinity and (a) winter-mean SIE over the Barents and northern Kara Seas and (b) winter-mean meridional wind averaged over the same area.

minimum salinity reached when the surface water attains the freezing temperature in winter. Additional ice formation might then increase the upper-layer salinity during the rest of the winter season. The role of sea ice forcing is also indicated by correlations between the 5-yr-lagged on-slope LHW salinity and the winter-mean SIE over the Barents and northern Kara Seas (Fig. 5a; $r = -0.60$) and the winter-mean meridional wind component averaged over the same area (Fig. 5b; $r = 0.41$), the latter two leading the LHW salinity. These correlations imply the following patterns of wind-driven regularities. Over the Barents and northern Kara Seas, wind from the south forces the sea ice toward the Arctic Ocean, resulting in a lower SIE. The reduced SIE indicates more open water and therefore the possibility for more brine release and increasing salinity due to more intensive formation of new sea ice. In periods when wind exports large amounts of ice out of the Barents Sea, the salinity of the water increases, and vice versa (Ellingsen et al. 2009). The 5-yr lag corresponds to an ~5-yr transit time for the Atlantic-origin water between the Barents and Laptev Seas on the basis of tracer analysis (Frank et al. 1998; Smith et al. 2011). Note that the time lagging outside 5 ± 1 yr exhibits no correlations.

Our results from a numerical simulation of water dynamics and salinity at 50-m depth identify the outflow from the northern Kara Sea as a potential source of the LHW salinity anomaly over the Laptev Sea continental slope, which is also in agreement with simulations by Maslowski et al. (2004) and Aksenov et al. (2011). Figure 6b shows a positive on-slope LHW salinity anomaly (by ~0.8) relative to the off slope that is consistent with the on-slope salinity anomaly derived from the field observations (Figs. 2a, 2b, and 3c). Sticks (LHW currents) suggest that this anomaly is associated with LHW outflow from the northern Kara Sea.

The realism of the simulations suggests a fair model capability in reproducing the basic hydrography. The time series of the simulated off-slope AW temperature, on-slope LHW temperature, and depth of the 0°C isotherm in the upper AW layer show no drift associated with model stability (Figs. 4a–c). In contrast, these time series show interdecadal variability that is qualitatively consistent with observational data (Figs. 4a–c). However, the upper boundary of the AW layer is found in the model higher in the water column than it is in the observations, along with higher off-slope AW-layer temperatures (Figs. 4a,b). This is a common problem shared by different model simulations of the Arctic Ocean (Holloway et al. 2007) and is likely related to limitations of the employed advection–diffusion schemes, resulting in excessive diffusion of tracers such as temperature and salinity. The variability of the AW layer and its circulation pattern (not shown) is, however, in the model really akin to observations.

Across the LHW, the model also shows on-slope LHW temperature and salinity anomalies that are qualitatively consistent with observations (cf. Figs. 2a and 2b and Fig. 6b). In the simulations, however, the on-slope salinities remain higher than the off-slope salinities at depths that exceed the LHW level defined by the observations (Fig. 6b). This is likely explained by the lack of eddy across-slope exchange at the employed resolution, deficiencies of the vertical mixing parameterization (e.g., excluded small-scale mixing processes), and lack of tidal mixing. All of these factors contribute to a conservation

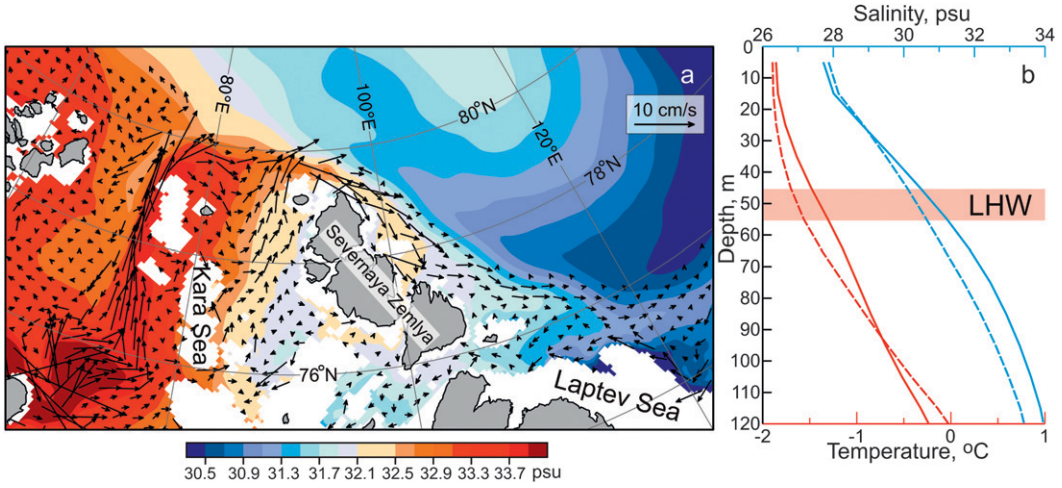

FIG. 6. (a) Simulated long-term mean (1970–2009) LHW (50 m) velocity and salinity demonstrate the saltier water inflow from the northern Kara Sea, propagating along the Laptev Sea continental slope. Sticks show currents over the depth range of the Laptev Sea continental slope from 150 to 2000 m. (b) Simulated long-term mean (1970–2009) vertical profiles of temperature (°C; red) and salinity (psu; blue) at 77.20°N (on slope; solid lines) and 78.50°N (off slope; dashed lines) in the central Laptev Sea at ~126°E. Pink shading indicates the depth range for the LHW.

of the on-slope LHW properties while translating along slope from the Barents and northern Kara Seas.

5. Summary

Our historical data analysis complemented by hydrodynamic modeling shows that an important proportion of the LHW salinity anomaly over the Laptev Sea continental slope is due to the Barents Sea branch (remote forcing), whereas the LHW temperature anomaly seems to be attributed to interaction with underlying AW (local forcing). Furthermore, our qualitative analysis suggests that the Barents Sea branch of LHW over the Laptev Sea continental margin is modified by upstream sea ice and atmospheric forcing. In this context, on-slope LHW warming of the late 2000s seems to be only in part due to warmer AW inflow. In the early 2000s, wind-forced reduction of SIE over the Barents Sea during winter could result in positive salinity anomalies that are being transported downstream along the Laptev Sea continental margin, reducing on-slope vertical salinity stratification and favoring vertical exchange with underlying warmer AW in the late 2000s. This development demonstrates that AW heat release may be enhanced by remote regional mechanisms and restricted to confined areas. Future climate change associated with further sea ice retreat over the Barents Sea during winter may bring more saline LHW onto the slope, favoring upward AW heat release.

Acknowledgments. We gratefully acknowledge financial support through the BMBF project "System Laptev Sea." BR was supported by the EU-THOR project. The numerical simulations were performed at the DKRZ, Hamburg, Germany, in the frame of the BMBF project "Nordatlantik" (WP 4.1). NVK is supported by the European Commission's Seventh Framework Programme through the MONARCH-A Collaborative Project, FP7-Space-2009-1 Contract 242446. This study also received financial support from the Canada Excellence Research Chair (CERC) program. Data analysis was also supported by the EU FP7 ACCESS project.

REFERENCES

Aksenov, Y., V. V. Ivanov, A. J. G. Nurser, S. Bacon, I. V. Polyakov, A. C. Coward, A. C. Naveira-Garabato, and A. Beszczynska-Moeller, 2011: The Arctic Circumpolar Boundary Current. *J. Geophys. Res.,* **116,** C09017, doi:10.1029/2010JC006637.

Arctic Climatology Project, 1997: Environmental Working Group joint U.S.–Russian atlas of the Arctic Ocean—Winter period. National Snow and Ice Data Center, Boulder, CO, CD-ROM.

——, 1998: Environmental Working Group joint U.S.-Russian atlas of the Arctic Ocean—Summer period. National Snow and Ice Data Center, Boulder, CO, CD-ROM.

Coachman, L. K., and K. Aagaard, 1974: Physical oceanography of the Arctic and sub-Arctic seas. *Marine Geology and Oceanography of the Arctic Seas,* Y. Herman, Ed., Springer-Verlag, 1–72.

Dmitrenko, I. A., I. V. Polyakov, S. A. Kirillov, L. A. Timokhov, H. L. Simmons, V. V. Ivanov, and D. Walsh, 2006: Seasonal variability of Atlantic Water on the continental slope of the Laptev Sea during 2002–2004. *Earth Planet. Sci. Lett.,* **244,** 735–743.

——, and Coauthors, 2008: Toward a warmer Arctic Ocean: Spreading of the early 21st century Atlantic Water warm anomaly along the Eurasian Basin margins. *J. Geophys. Res.,* **113,** C05023, doi:10.1029/2007JC004158.

——, D. Bauch, S. A. Kirillov, N. Koldunov, P. J. Minnette, V. V. Ivanov, J. A. Hölemann, and L. A. Timokhov, 2009: Barents Sea upstream events impact the properties of Atlantic Water inflow into the Arctic Ocean: Evidence from 2005 to 2006 downstream observations. *Deep-Sea Res. I,* **58,** 513–527.

——, V. V. Ivanov, S. A. Kirillov, E. L. Vinogradova, S. Torres-Valdes, and D. Bauch, 2011: Properties of the Atlantic derived halocline waters over the Laptev Sea continental margin: Evidence from 2002 to 2009. *J. Geophys. Res.,* **116,** C10024, doi:10.1029/2011JC007269.

Ellingsen, I., D. Slagstad, and A. Sundfjord, 2009: Modification of water masses in the Barents Sea and its coupling to ice dynamics: A model study. *Ocean Dyn.,* **59,** 1095–1108.

Frank, M., W. M. Smethie Jr., and R. Bayer, 1998: Investigation of subsurface water flow along the continental margin of the Eurasian Basin using the transient tracers tritium, ^{3}He, and CFCs. *J. Geophys. Res.,* **103,** 30 773–30 792.

Gouretski, V. V., and K. P. Koltermann, 2004: WOCE Global Hydrographic Climatology. Bundesamt für Seeschifffahrt und Hydrographie Rep. 35, 52 pp.

Holloway, G., and Coauthors, 2007: Water properties and circulation in Arctic Ocean models. *J. Geophys. Res.,* **112,** C04S03, doi:10.1029/2006JC003642.

Kalnay, E., and Coauthors, 1996: The NCEP/NCAR 40-Year Reanalysis Project. *Bull. Amer. Meteor. Soc.,* **77,** 437–471.

Marshall, J., A. Adcroft, C. Hill, L. Perelman, and C. Heisey, 1997: A finite-volume, incompressible Navier Stokes model for studies of the ocean on parallel computers. *J. Geophys. Res.,* **102,** 5753–5766.

Maslowski, W., D. Marble, W. Walczowski, U. Schauer, J. L. Clement, and A. J. Semtner, 2004: On climatological mass, heat, and salt transports through the Barents Sea and Fram Strait from a pan-Arctic coupled ice-ocean model simulation. *J. Geophys. Res.,* **109,** C03032, doi:10.1029/2001JC001039.

Polyakov, I. V., D. Walsh, I. Dmitrenko, R. L. Colony, and L. A. Timokhov, 2003: Arctic Ocean variability derived from historical observations. *Geophys. Res. Lett.,* **30,** 1298, doi:10.1029/2002GL016441.

——, and Coauthors, 2004: Variability of the intermediate Atlantic Water of the Arctic Ocean over the last 100 years. *J. Climate,* **17,** 4485–4497.

——, and Coauthors, 2010: Arctic Ocean warming contributes to reduced polar ice cap. *J. Phys. Oceanogr.,* **40,** 2743–2756.

Rudels, B., 2010: Constraints on exchanges in the Arctic Mediterranean—Do they exist and can they be of use? *Tellus,* **62A,** 109–122.

——, L. G. Anderson, and E. P. Jones, 1996: Formation and evolution of the surface mixed layer and the halocline of the Arctic Ocean. *J. Geophys. Res.,* **101,** 8807–8821.

——, E. P. Jones, U. Schauer, and P. Eriksson, 2004: Atlantic sources of the Arctic Ocean surface and halocline waters. *Polar Res.,* **23,** 181–208.

Serra, N., R. H. Käse, A. Köhl, D. Stammer, and D. Quadfasel, 2010: On the low-frequency phase relation between the Denmark Strait and the Faroe-Bank Channel overflows. *Tellus,* **62A,** 530–550.

Smith, J. N., F. A. McLaughlin, W. M. Smethie Jr., S. B. Moran, and K. Lepore, 2011: Iodine-129, ^{137}Cs, and CFC-11 tracer transit time distributions in the Arctic Ocean. *J. Geophys. Res.,* **116,** C04024, doi:10.1029/2010JC006471.

Steele, M., J. Morison, and T. Curtin, 1995: Halocline water formation in the Barents Sea. *J. Geophys. Res.,* **100** (C1), 881–894.